TECHNISCHE MECHANIK, 32, 2-5, (2012), 251– 264
submitted: September 29, 2011

Numerical Multiscale Modelling of Sandwich Plates

C. Helfen, S. Diebels

Sandwich plates present a complicated material behaviour, strongly depending on the considered materials and on the layer composition. Therefore, it is an increasing interest to feature a model of their mechanical behaviour. A multiscale model is developed in the paper. In the scope of this project, some layers show non-linear material behaviour at large strains and, as a consequence, the classical plate theory cannot be considered. At this stage, only linear elastic material behaviour and small deformations are taken into account, in order to validate the presented model; but to guaranty the possibility to consider non-linear material behaviour, a numerical homogenisation is chosen explicitly taking into account the stacking order and the material behaviour of the individual layers.

A numerical homogenisation, or so-called FE^2, consists of a Finite Element computation on a macroscale -here a plate which contains the plate kinematics and balance equations; but instead of applying the constitutive equations on this scale, the deformations are projected on a mesoscale where the mesostructure is fully resolved and another Finite Element computation is performed on this level. In this paper, a plate theory following Mindlin concept with five degrees of freedom is considered on the macroscale, and a three dimensional boundary value problem is solved in the mesoscale resolving the stacking order of the sandwich. Whereas the macroscale problem is implemented in a non-commercial FORTRAN code, the mesoscale is modelled using the commercial software ABAQUS® and an UMAT SUBROUTINE. In order to find an analytical tangent for the global iterations, a Multi-Level Newton Algorithm is applied, which enables a faster computation.

1 Introduction

Composites plates are nowadays widely used because of their outstanding mechanical properties, especially for transport industries like airplane and automotive industries. However, they are quite difficult to test experimentally, hence there exists an increasing interest for modelling. To model the mechanical behaviour of sandwich plates, one can basically use the classical plate theory (or one of its derivatives), or any homogenisation strategy. Since some of the considered layers of the sandwich plate are metallic and show elasto-plastic material behaviour, the plate theory is not sufficient. To the knowlegde of the authors, no correct developments of the plate theory have been made that take into account non-linear material behaviour, cf. Altenbach (1988); Altenbach et al. (2010). Indeed the plate theory is unable to take into account non-linear material behaviour, like for instance plasticity. However, in this paper, only elastic material behaviour and small deformations are considered, in order to validate the presented model. But because of the need in a further work to consider elasto-plastic material behaviour, a multi-scale approach and more precisely a numerical homogenisation is used in the scope of this work, in order to predict the effective material behaviour of the sandwich plate taking into account an arbitrary stacking order and non-linear material behaviour of the layers.

In the considered numerical multi-scale method, the macroscale is computed as a plate and therefore contains the plate kinematics. For a better estimation of the shear stresses, a plate theory following Mindlin concept is considered, which has five degrees of freedom, i. e. three translations of a point located on the midplane and two rotations of the cross-sections. The transfer of the deformations from the macroscale to the mesoscale is made by a projection of the macroscopic deformation on the boundaries of a three dimensional volume on the mesoscale. In this context, the volume takes the whole plate thickness into account and - as a consequence for a sandwich plate - the different layers and their stacking order. On this level, a representative volume element (RVE) is defined, and a mesoscopic boundary value problem is solved. Forces and moments are then calculated as resultants of the mesoscale computation and transferred back to the macroscale.

The first multi-scale modelling was done by Castaneda (2002a,b) and Suquet (1985). Further developments in the scope of a numerical homogenisation were presented, e.g., by Schröder et al. (1999), Feyel and Chaboche (2000); Feyel (2001, 2003) and Kouznetsova (2002); Kouznetsova et al. (2004). Recently, a second order or Cosserat theory is used, in order to improve the technique by considering complex heterogeneities, cf. Forest (1998, 2002); Forest and Trinh (2011), Kouznetsova et al. (2001), and Larsson and Diebels (2007) and Jänicke and Diebels (2010a,b); Jänicke et al. (2009). For the specific case of plates, an analytical homogenisation was first used by Laschet et al. (1989) and Hohe (2003). Later on, a numerical homogenisation was also studied for this kind of materials, cf. Geers et al. (2007); Coenen et al. (2010); Landervik and Larsson (2008).

Within the framework of this paper, an FE^2 approach is applied and an analytical tangent is defined with the help of a Multi-Level Newton Algorithm, cf. Ellsiepen and Hartmann (2001); Hartmann (2005); Hartmann et al. (2008). The procedure is the same as the global-local iteration in the case of constitutive equations of evolutionary type (viscoelasticity, elasto-plasticity or viscoplasticity). The same way of thinking can be applied for a numerical homogenisation, in order to identify an accurate tangent stiffness. Whereas most of the authors working on FE^2 are using a numerical tangent, what considerably slows down the computations, we will use an analytical tangent for sake of efficiency.

In the next chapter, the principle of a FE^2 is shown in details: the plate kinematics on the macroscale is given, followed by the possible projections rules. Then the boundary value problem, solved on the mesoscale, is exposed. Lastly, the transfer of the stress and moment resultants from the mesoscale to the macroscale is explained. In the fourth chapter, a Multi-Level-Newton Algorithm is presented, in order to define the analytical tangent. In the fifth chapter, the results for a single layer plate, as well as for a sandwich plate are presented in case of traction, shear and bending tests.

2 Principle of a Numerical Homogenisation of Composites Plates

In this section, the homogenisation method used for the sandwich plate is introduced. The components of the macroscale are written in capital letters for the displacements or with the index $(.)_M$ for the stress resultants, whereas the components of the mesoscale are defined with lower case letters for the displacements or with the index $(.)_m$. The principle of a numerical homogenisation for plates is explained in Figure 1 and can be divided in four steps.

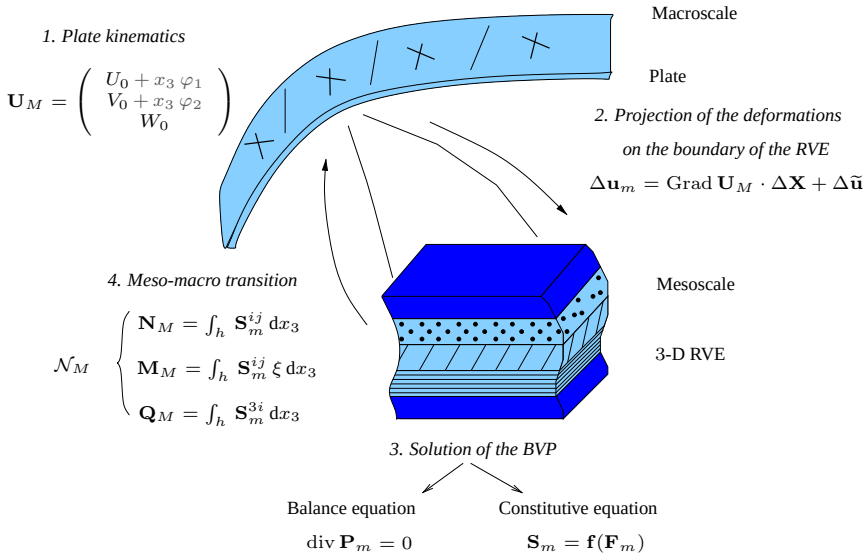

Figure 1: Principle of a numerical homogenisation of plates

1. The first step is related to the macroscale. In the scope of this work, a plate theory with five degrees of freedom is used. The plate kinematics are defined and the equilibrium equations are solved using a FEM discretisation of the plate.

2. The projection of the deformations from the macroscale on the boundary of the representative volume element on the mesoscale consists of the second step defining an additional boundary value problem on the mesoscale. At each integration point of the macroscale an individual RVE is attached.

3. Then the boundary value problem on the mesoscale is solved with the balance equations and the constitutive equations. An advantage of this technique is the possibility to consider any three dimensional constitutive law without any further transformations of it, and to take into account an arbitrary stacking order of the sandwich plate.

4. The last step is related to the determination of the stress and moment resultants for the macroscale, which are computed from the local stress distribution obtained from the boundary value problem on the mesoscale.

In the next subsections, the four steps will be explained in detail.

2.1 Macroscale: Plate Kinematics

In the context of this work, a classical plate theory of Mindlin type is used, cf. Altenbach et al. (1996); Reddy (1997). It contains five degrees of freedom: U_0, V_0, W_0 are the three translational degrees of freedom, whereas φ_1, φ_2 are the two rotational degrees of freedom. The 5-degrees of freedom plate theory corresponds to a Cosserat theory for plates, as illustrated in Altenbach et al. (2010).

As a result, the local displacement field over the plate's thickness is expressed as

$$\begin{aligned} U &= U_0 + x_3\,\varphi_1, \\ V &= V_0 + x_3\,\varphi_2, \\ W &= W_0, \end{aligned} \tag{1}$$

where x_3 is the thickness (or out-of-plane) coordinate and is by convention defined as zero in the mid plane. For clarity, the first order components are written in gray.

The in-plane deformations are also defined as

$$\varepsilon_{11} = \varepsilon_{11}^0 + x_3\,\kappa_{11} = \frac{\partial U_0}{\partial x_1} + x_3\,\frac{\partial \varphi_1}{\partial x_1}, \tag{2}$$

$$\varepsilon_{22} = \varepsilon_{22}^0 + x_3\,\kappa_{22} = \frac{\partial V_0}{\partial x_2} + x_3\,\frac{\partial \varphi_2}{\partial x_2}, \tag{3}$$

where by definition the coordinates (x_1, x_2) are the in-plane coordinates. Thus, the in-plane shear deformation is defined as

$$\varepsilon_{12} = \varepsilon_{12}^0 + x_3\,\kappa_{12} = \frac{1}{2}\left(\frac{\partial U_0}{\partial x_2} + \frac{\partial V_0}{\partial x_1}\right) + x_3\,\frac{1}{2}\left(\frac{\partial \varphi_1}{\partial x_2} + \frac{\partial \varphi_2}{\partial x_1}\right), \tag{4}$$

whereas the out-of-plane shear deformations

$$\boldsymbol{\gamma}_3 = \left\{ \begin{array}{l} \varepsilon_{13} = \varepsilon_{13}^0 = \frac{1}{2}\left(\dfrac{\partial W_0}{\partial x_1} + \varphi_1\right), \\ \varepsilon_{23} = \varepsilon_{23}^0 = \frac{1}{2}\left(\dfrac{\partial W_0}{\partial x_2} + \varphi_2\right), \end{array} \right. \tag{5}$$

are not dependent on the coordinate in transverse direction. In the framework of the plate theory with five degrees of freedom, the deformation in thickness direction ε_{33} is neglected in relation with ε_{11} and ε_{22}, cf. Altenbach et al. (1996).

We also define the stress resultants on the macroscale $\mathcal{N}_M$, i. e. the normal force $\mathbf{N}_M$, moment $\mathbf{M}_M$, and shear force $\mathbf{Q}_M$ as the integration of the stress distribution and its first moment across the plate thickness as

$$\mathcal{N}_M = [\mathbf{N}_M, \mathbf{M}_M, \mathbf{Q}_M]^T = \int_{-h/2}^{h/2} [\mathbf{P}_m^{ij}, \mathbf{P}_m^{ij}\,x_3, \mathbf{P}_m^{3i}]^T \,\mathrm{d}x_3, \qquad (i,j) = (1,2) \tag{6}$$

where $\mathbf{P}_m$ is the mesoscopic 1^{st} Piola-Kirchhoff stress tensor. The five equilibrium equations are thus defined on the macroscale as, cf. Reddy (1990, 1997), when no external load is applied

$$\mathbf{G} = \begin{bmatrix} N_{11,1} + N_{12,2} \\ N_{12,1} + N_{22,2} \\ Q_{1,1} + Q_{2,2} \\ M_{11,1} + M_{12,2} - Q_1 \\ M_{12,1} + M_{22,2} - Q_2 \end{bmatrix} = \mathbf{0}. \tag{7}$$

For the use of a FE^2 method for plates, kinematic relations for the plate have to be defined. The major difference with the classical plate theory is that the constitutive law is not modified according to the kinematic assumptions like for the plate theory, but on each Gauss point of the macroscopic FE discretisation, the deformations are projected on a three dimensional mesoscale volume. In the mesoscale, a separate Finite Element computation of the mesostructure problem is performed; and the results are transferred back to the macroscale in terms of the stress resultants. The constitutive law is then defined within the mesoscale problem, i. e., in a local 3-dimensional problem. As a consequence, two major advantages occur: firstly, the constitutive law has not to be changed in order to pass the plate kinematics; secondly, any constitutive law can be used, even non-linear ones. On the one hand, the major drawback of this kind of theory lies in the high computational costs, which, however, can be dramatically reduced due to parallelisation.

2.2 Projection Rules

There are different possibilities to project the deformations on the mesoscale, Kouznetsova (2002); Coenen et al. (2010):

- the Taylor or Voigt assumption, in which a constant deformation is projected to the mesoscale,
- the Sachs or Reuss assumption, in which a constant stress is projected to the mesoscale.

The Taylor assumption leads to an overestimation of the results in terms of the effective stiffness, whereas the Sachs assumption leads to an underestimation of the results. Both assumptions cannot be accurately used for sandwich structures, since neither the stresses nor the strains are homogeneous in a sandwich composite.

Another possibility - which is preferred in most of the cases because of its efficiency - is to project the deformations on the boundaries of the RVE taking into account an additional fluctuation field. We choose a projection on the nodes of the element, and the mesoscopic deformations $\Delta\mathbf{u}$ are defined as

$$\Delta\mathbf{u} = \mathrm{Grad}\,\mathbf{U} \cdot \Delta\mathbf{X} + \Delta\widetilde{\mathbf{u}} \tag{8}$$

where $\Delta\widetilde{\mathbf{u}}$ is chosen as periodic on opposite boundaries, written as

$$\mathbf{x}^+ - \mathbf{x}^- = \mathbf{F}_M \cdot (\mathbf{X}^+ - \mathbf{X}^-), \tag{9}$$

where the index $(\cdot)^+$ accounts for the front panel of the RVE and the index $(\cdot)^-$ for the opposite side. The deformations are assumed to be periodic, since the mesoscopic fluctuations of two parallel sides of an unit cell are identical.

The macroscopic deformation gradient is defined as the volume average of the mesoscopic deformation gradient

$$\mathbf{F}_M = \frac{1}{\mathcal{V}_0} \int_{\mathcal{V}_0} \mathbf{F}_m \, \mathrm{d}\mathcal{V}_0. \tag{10}$$

2.3 RVE

In the mesoscale, a 3-dimensional Representative Volume Element (RVE) is defined, which takes into account the stacking order of the different layers of the sandwich plate. Since the order of magnitude in the thickness direction is not much smaller in the mesoscale than in the macroscale, no homogenisation can be done in this direction. For

this reason, the numerical homogenisation is only done in two directions. In the thickness direction, no homogenisation is possible and a full resolution of the materials occurs. Furthermore, we choose a plate theory of Mindlin type which means that no thickness change occurs. In the present paper, a sandwich plate is studied, i. e. the structure is composed of three layers of different materials; whereas the core material is thick and has a low elastic modulus, the top panels are thin and stiff. It is to differentiate with laminates, which contains different layers of the same thickness and materials, but with different fibers orientations. However, the presented FE^2 method has the advantage to consider laminates plates as well as sandwich plates.

On the mesoscale, the balance equation between the internal and external work

$$\int_{\mathcal{V}_0} \mathbf{P}_m^T : \delta\mathbf{F}_m \, \mathrm{d}\mathcal{V}_0 - \int_{\partial\mathcal{V}_0} \mathbf{t} \cdot \delta\mathbf{x} \, \mathrm{d}\mathcal{V}_0 = 0 \tag{11}$$

as well as the local constitutive equation

$$\mathbf{P}_m = \mathcal{F}(\mathbf{F}_m) \tag{12}$$

apply, where $\mathbf{P}_m$ is the mesoscopic 1^{st} Piola-Kirchhoff stress tensor and $\mathbf{F}_m$ the mesoscopic deformation gradient. In contrast to the classical plate theory, even non-linear constitutive equations can be considered, like for example for elasto-plasticity. Furthermore, the constitutive equations do not need any further transformations, like it is the case for a 5-degrees of freedom plate theory.

2.4 Macro-Meso Transition

The Hill-Mandel condition, cf. Larsson and Diebels (2007) for a classical numerical homogenisation, postulates the equivalence of the macroscopic and the mesoscopic stress power

$$\frac{1}{\mathcal{V}_0} \int_{\mathcal{V}_0} \mathbf{P}_m : \delta\mathbf{F}_m^T \, \mathrm{d}V_0 = \mathbf{P}_M : \delta\mathbf{F}_M^T. \tag{13}$$

In order to fit into the plate kinematics of the macroscale, the Hill-Mandel condition is modified

$$\begin{aligned} \frac{1}{\mathcal{S}_0} \int_{\mathcal{V}_0} \mathbf{P}_m : \delta\mathbf{F}_m^T \, \mathrm{d}\mathcal{V}_0 \quad = \quad & \int_{\mathcal{S}} [\delta U_{0,1} \, N_{11} + (\delta U_{0,2} + \delta V_{0,1}) \, N_{12} + \delta V_{0,2} \, N_{22} \\ & + \delta W_{0,1} \, Q_1 + \delta W_{0,2} \, Q_2 + \delta\varphi_{1,1} \, M_{11} + (\delta\varphi_{1,2} + \delta\varphi_{2,1}) \, M_{12} \\ & + \delta\varphi_{2,2} \, M_{22} + \delta\varphi_1 \, Q_1 + \delta\varphi_2 \, Q_2] \, \mathrm{d}\mathcal{S}. \end{aligned} \tag{14}$$

However, the stress resultants are obtained from

$$\begin{aligned} \mathbf{N}_N &= \overset{4}{\mathbb{C}}_1 : \boldsymbol{\varepsilon}^0 + \overset{4}{\mathbb{C}}_2 : \boldsymbol{\kappa} + \overset{3}{\mathbb{C}}_4 \cdot \boldsymbol{\gamma}_3, \\ \mathbf{M}_M &= \overset{4}{\mathbb{C}}_2 : \boldsymbol{\varepsilon}^0 + \overset{4}{\mathbb{C}}_3 : \boldsymbol{\kappa} + \overset{3}{\mathbb{C}}_5 \cdot \boldsymbol{\gamma}_3, \\ \mathbf{Q}_M &= \overset{3}{\mathbb{C}}_4 : \boldsymbol{\varepsilon}^0 + \overset{3}{\mathbb{C}}_5 : \boldsymbol{\kappa} + \overset{2}{\mathbb{C}}_6 \cdot \boldsymbol{\gamma}_3, \end{aligned} \tag{15}$$

where $\mathbf{N}_N$ is the second order force tensor, $\mathbf{M}_M$ is the second order moment tensor and $\mathbf{Q}_M$ is the shear stress vector. The $\overset{j}{\mathbb{C}}_i$ are the tangent stiffness, which are tensors of order j, used for an analytical tangent within the FE^2 approach; the determination of them will be shown in the next chapter.

3 Multi-Level Newton Algorithm (MLNA)

3.1 Principle of the MLNA

The difficulty applying an FE^2 model consists of the determination of an accurate tangent stiffness for the macroscale (that is the plate) from the mesoscale (the 3-dimensional problem). To solve this issue, we will use a Multi-Level

Newton Algorithm, firstly used by Rabat et al. Rabbat et al. (1979) for electrical networks, later on by Ellsiepen and Ellsiepen and Diebels (2001) for the solution of mechanical problems when the constitutive law is of evolutionary type. For these issues, the principle of a MLNA is to separate the two systems of equations in one global system, which contains the equilibrium equations, and one local system, which consists of the evolution equations. The same kind of procedure can be used for FE^2, cf. Hartmann et al. (2008), in which the macroscale is represented by the global level and the mesoscale by the local level.

The discretised system of the equilibrium equations $\mathbf{G}\left(\mathcal{N}_M\right)$, see equation (7), represents the global level, whereas the local level consists of the 3-dimensional boundary value problem of the mesoscale defined at each macroscopic integration point. In the local level, the problem will be subdivided in two parts: one on the boundary $\mathbf{l}^\Gamma$ of the RVE - which is obtained by the projection - and the other inside the RVE $\mathbf{l}^\Omega$, which corresponds to the local equilibrium

$$\mathbf{l} = \begin{pmatrix} \mathbf{l}^\Gamma \\ \\ \mathbf{l}^\Omega \end{pmatrix} = \begin{pmatrix} \Delta\mathbf{u}^\Gamma - \operatorname{Grad}\mathbf{U}_M \cdot \Delta\mathbf{X} \\ \\ \operatorname{div}\boldsymbol{\sigma}\left(\mathbf{u}^\Omega, \mathbf{u}^\Gamma\right) \end{pmatrix} = \mathbf{0}. \tag{16}$$

Thus, the displacements of the local problem are divided into an unknown and a known (prescribed) part, as represented in figure 2. $\mathbf{u}^\Omega$ is the unknown part, inside the RVE and $\mathbf{u}^\Gamma$ is the prescribed part, on the boundary of the RVE Hartmann et al. (2008).

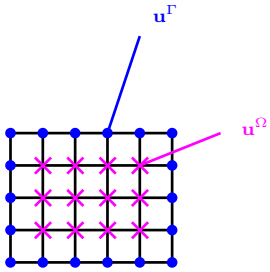

Figure 2: Schematic representation of the displacement on the local level: on the boundary ($\mathbf{u}^\Gamma$) and inside the element ($\mathbf{u}^\Omega$)

Then a discretisation is made by multiplication with a test function and integration over the volume. The equilibrium equations of the macroscale (7) become

$$\mathbf{G} = \begin{bmatrix} \int_S \left[\delta U_{0,1}\, N_{11} + \delta U_{0,2}\, N_{12}\right] \mathrm{d}x\mathrm{d}y - \oint_s \mathcal{P}_1\, \delta U_0\, \mathrm{d}s \\ \int_S \left[\delta V_{0,1}\, N_{12} + \delta V_{0,2}\, N_{22}\right] \mathrm{d}x\mathrm{d}y - \oint_s \mathcal{P}_2\, \delta U_0\, \mathrm{d}s \\ \int_S \left[\delta W_{0,1}\, Q_1 + \delta W_{0,2}\, Q_2 - \delta W_0\, q + \mathcal{N}_1\right] \mathrm{d}x\mathrm{d}y - \oint_s \mathcal{Q}\, \delta U_0\, \mathrm{d}s \\ \int_S \left[\delta\varphi_{1,1}\, M_{11} + \delta\varphi_{1,2}\, M_{12} + \delta\varphi_1\, Q_1\right] \mathrm{d}x\mathrm{d}y - \oint_s \mathcal{T}_1\, \delta U_0\, \mathrm{d}s \\ \int_S \left[\delta\varphi_{2,1}\, M_{12} + \delta\varphi_{2,2}\, M_{22} + \delta\varphi_2\, Q_2\right] \mathrm{d}x\mathrm{d}y - \oint_s \mathcal{T}_2\, \delta U_0\, \mathrm{d}s \end{bmatrix} = \mathbf{0}, \tag{17}$$

where, cf. Reddy (1997)

$$\begin{aligned} \mathcal{P}_1 &= N_{11}\, n_1 + N_{12}\, n_2, \\ \mathcal{P}_1 &= N_{12}\, n_1 + N_{22}\, n_2, \\ \mathcal{N}_1 &= \delta W_{0,1}\left(N_{11}\, W_{0,1} + N_{12}\, W_{0,2}\right) + \delta W_{0,2}\left(N_{12}\, W_{0,1} + N_{22}\, W_{0,2}\right), \\ \mathcal{Q} &= \left(Q_1 + N_{11}\, W_{0,1} + N_{12}\, W_{0,2}\right) n_1 + \left(Q_2 + N_{11}\, W_{0,1} + N_{22}\, W_{0,2}\right) n_2, \\ \mathcal{T}_1 &= M_{11}\, n_1 + M_{12}\, n_2, \\ \mathcal{T}_2 &= M_{12}\, n_1 + M_{22}\, n_2, \end{aligned} \tag{18}$$

and $\mathbf{n}$ is defined as the unit vector normal and $\mathbf{n} = [n_1, n_2]^T$. A discretisation of the equilibrium equation of the

mesoscale (16 a) is based on the weak form of the equilibrium condition

$$\int_{\mathcal{B}_0} \delta\mathbf{u} : \boldsymbol{\sigma}\, \mathrm{d}\mathcal{B}_0 - \int_{\partial\mathcal{B}_0} \delta\mathbf{u} \cdot \mathbf{t}\, \mathrm{d}\partial\mathcal{B}_0 = 0$$

After a discretization, it follows for the deformations on the local level

$$\boldsymbol{\varepsilon} \;=\; \sum_{k=1}^{n^\Gamma} \mathbf{B}_k^\Gamma\, \mathbf{u}_k^\Gamma + \sum_{k=1}^{n^\Omega} \mathbf{B}_k^\Omega\, \mathbf{u}_k^\Omega, \tag{19}$$

where $\mathbf{u}_k$ is the nodal displacement at node k and the $\mathbf{B}_k$ are the derivatives of the shape functions. The virtual deformations are defined as

$$\delta\boldsymbol{\varepsilon} = \sum_{k=1}^{n^\Omega} \mathbf{B}_k^\Omega\, \delta\mathbf{u}_k^\Omega, \tag{20}$$

since the virtual displacement on the boundary vanishes

$$\delta\mathbf{u}^\Gamma = 0. \tag{21}$$

Subsequently for the macro-meso problem, it returns to solve the following 2-levels system

$$\begin{bmatrix} \mathbf{G} \\ \mathbf{l} \end{bmatrix} = - \begin{bmatrix} \mathbf{R}_\mathbf{U} \\ \mathbf{R}_\mathbf{u} \end{bmatrix} = \mathbf{0}, \tag{22}$$

composed of the global level (the plate), and the local level, containing the 3-dimensional Finite Element computation of the RVE. In order to solve this system, a Newton iteration is required

$$\left[\begin{array}{c|c} \dfrac{\partial\mathbf{G}}{\partial\mathbf{U}} & \dfrac{\partial\mathbf{G}}{\partial\mathbf{u}} \\ \hline \dfrac{\partial\mathbf{l}}{\partial\mathbf{U}} & \dfrac{\partial\mathbf{l}}{\partial\mathbf{u}} \end{array}\right] \cdot \left[\begin{array}{c} \mathrm{d}\mathbf{U} \\ \hline \mathrm{d}\mathbf{u} \end{array}\right] = - \left[\begin{array}{c} \mathbf{R}_\mathbf{U} \\ \hline \mathbf{R}_\mathbf{u} \end{array}\right]. \tag{23}$$

The partitioning of the Jacobian is with respect to the MLNA. The system (22) is solved in a Newton iteration in 3 steps, cf. Hartmann et al. (2008):

- Step 1: In the first step, the local level is considered, therefore the global displacement is assumed to be known ($\mathrm{d}\mathbf{U} = \mathbf{0}$). The second line of the system (23) can be simplified as

  $$\frac{\partial\mathbf{l}}{\partial\mathbf{u}} \cdot \mathrm{d}\mathbf{u} = -\mathbf{R}_\mathbf{u}, \tag{24}$$

  which leads to the determination of $\mathrm{d}\mathbf{u}$.

- Step 2: In the second step, an update of the local variable $\mathbf{u}$ is done, and we now return to the global level. We assume that an equilibrium is found on the local level, and thus the residuum is set to zero

  $$\mathbf{R}_\mathbf{u} = 0. \tag{25}$$

  By considering the second line of the system (23), we can determine a relation between the local increment $\mathrm{d}\mathbf{u}$ and the global increment $\mathrm{d}\mathbf{U}$

  $$\frac{\partial\mathbf{l}}{\partial\mathbf{U}} \cdot \mathrm{d}\mathbf{U} + \frac{\partial\mathbf{l}}{\partial\mathbf{u}} \cdot \mathrm{d}\mathbf{u} = \mathbf{0}, \tag{26}$$

  which leads to a direct relation between the global increments and the local displacements

  $$\mathrm{d}\mathbf{u} = \left(\frac{\partial\mathbf{l}}{\partial\mathbf{u}}\right)^{-1} \cdot \left(-\frac{\partial\mathbf{l}}{\partial\mathbf{U}}\right) \cdot \mathrm{d}\mathbf{U}. \tag{27}$$

- Step 3: In the last step, the first line of the system (23) is solved on the global level taking into account (27)

$$\frac{\partial \mathbf{G}}{\partial \mathbf{U}} \cdot \mathrm{d}\mathbf{U} + \frac{\partial \mathbf{G}}{\partial \mathbf{u}} \cdot \mathrm{d}\mathbf{u} = \left(\frac{\partial \mathbf{G}}{\partial \mathbf{U}} + \frac{\partial \mathbf{G}}{\partial \mathbf{u}} \cdot \frac{\mathrm{d}\mathbf{u}}{\mathrm{d}\mathbf{U}} \right) \cdot \mathrm{d}\mathbf{U} = -\mathbf{R}_{\mathbf{U}}, \tag{28}$$

where some simplifications can be done: the global level does not depend directly on the macroscopic increments, that leads to

$$\frac{\partial \mathbf{G}}{\partial \mathbf{U}} = \mathbf{0}. \tag{29}$$

Hence, the equation (28) reduces to

$$\left(\frac{\partial \mathbf{G}}{\partial \mathbf{u}} \cdot \frac{\mathrm{d}\mathbf{u}}{\mathrm{d}\mathbf{U}} \right) \cdot \mathrm{d}\mathbf{U} = -\mathbf{R}_{\mathbf{U}}. \tag{30}$$

From this equation, one can identify the tangent stiffness $\mathbf{K}$ as $\mathbf{K} \cdot \mathrm{d}\mathbf{U} = -\mathbf{R}_{\mathbf{U}}$

$$\mathbf{K} \quad = \quad \left(\frac{\partial \mathbf{G}}{\partial \mathbf{u}} \cdot \frac{\mathrm{d}\mathbf{u}}{\mathrm{d}\mathbf{U}} \right), \tag{31}$$

and according to the chain rule

$$\mathbf{K} \quad = \quad \frac{\partial \mathbf{G}}{\partial \mathcal{N}_M} \cdot \frac{\partial \mathcal{N}_M}{\partial \mathbf{u}} \cdot \frac{\mathrm{d}\mathbf{u}}{\mathrm{d}\mathbf{U}}, \tag{32}$$

taking into account the explicit dependences of $\mathbf{G}$ on the macroscopic stress resultants $\mathbf{N}_M$.

3.2 Application to FE^2

The macroscopic tangent stiffness is decomposed according to the chain rule, in order to use the dependence of the mesoscopic stresses on the mesoscopic deformations

$$\frac{\partial \mathcal{N}_M}{\partial \varepsilon_M} = \frac{\partial \mathcal{N}_M}{\partial \boldsymbol{\sigma}_m} \cdot \frac{\partial \boldsymbol{\sigma}_m}{\partial \boldsymbol{\varepsilon}_m} \cdot \frac{\partial \boldsymbol{\varepsilon}_m}{\partial \boldsymbol{\varepsilon}_M} \tag{33}$$

where $\boldsymbol{\varepsilon}_M$ is defined as containing the whole macroscopic deformations and $\boldsymbol{\varepsilon}_m$ as the mesoscopic deformations. From the definitions of the macroscopic stress resultants as a function of the mesoscopic stresses, from the classical plate theory

$$\mathcal{N}_M^T = [N_{ij}, M_{ij}, Q_i]^T = \int_{-h/2}^{h/2} [\sigma_m^{ij}, \sigma_m^{ij}\, x_3, \sigma_m^{3i}]^T \, \mathrm{d}x_3, \qquad (i,j) = (1,2),$$

we can find a direct relation between the macroscopic forces and the mesoscopic stresses, in the linear case

$$N_{ij} = \int_{-h/2}^{h/2} \sigma_m^{ij} \, \mathrm{d}x_3 = \int_{-h/2}^{h/2} \sum_{k,l} \mathbb{C}_{ijkl}\, \varepsilon_{m\,kl} \, \mathrm{d}x_3 = \sum_{p,k,l} \mathbb{C}^p_{ijkl}\, \varepsilon^p_{m\,kl}\ h, \tag{34}$$

where the macroscopic stress resultant is equal to the sum over the elements of the mesoscopic stresses multiplied by the thickness of the plate. $\mathbb{C}$ is defined as the elastic tensor of the mesoscopic model, $\boldsymbol{\sigma} = \mathbb{C} : \boldsymbol{\varepsilon}$ and $\mathbb{C} = \partial \mathbf{l} / \partial \boldsymbol{\varepsilon}$. $\sum_{p,k,l}$ is defined as the sum over the indices p, k, l; k and l are the sum index and $k, l = 1, 3$; p is the index over the thickness of the RVE. The same principle applies for the moment

$$M_{ij} = \int_{-h/2}^{h/2} \sigma_m^{ij}\, x_3 \, \mathrm{d}x_3 = \sum_{p,k,l} \mathbb{C}^p_{ijkl}\, \varepsilon^p_{m\,kl}\, x_3\ h, \tag{35}$$

and the shear stresses

$$Q_i = \int_{-h/2}^{h/2} \sigma_m^{3i} \, \mathrm{d}x_3 = \sum_{p,k,l} \mathbb{C}^p_{3ikl}\, \varepsilon^p_{m\,kl}\ h. \tag{36}$$

The relation between the macroscopic and mesoscopic deformation is also needed

$$\boldsymbol{\varepsilon}_M = \left\{ \begin{array}{cc} \boldsymbol{\varepsilon}^0_M + x_3\,\boldsymbol{\kappa}_M & ij = 11, 12, 22 \\ \boldsymbol{\gamma}_3 & ij = 13, 23 \end{array} \right\} = \frac{1}{\mathcal{V}_0} \int_{\mathcal{V}_0} \boldsymbol{\varepsilon}_m \mathrm{d}\mathcal{V}_0. \tag{37}$$

Thus, we obtain the tangent stiffness

$$\mathcal{N}_M = \left[\begin{array}{c} \mathbf{N} \\ \mathbf{M} \\ \mathbf{Q} \end{array} \right] = \mathbb{C}_M : \boldsymbol{\varepsilon}_M = \mathbb{C}_M : \left[\begin{array}{c} \boldsymbol{\varepsilon}^0 \\ \boldsymbol{\kappa} \\ \boldsymbol{\gamma}_3 \end{array} \right], \tag{38}$$

with $\mathbb{C}_M$

$$\mathbb{C}_M = \left[\begin{array}{ccc} \sum_p \mathbb{C}^p_{ijkl}\, h & \sum_p \mathbb{C}^p_{ijkl}\, h\, x_3 & 0 \\ \sum_p \mathbb{C}^p_{ijkl}\, h\, x_3 & \sum_p \mathbb{C}^p_{ijkl}\, h\, x_3^2 & 0 \\ 0 & 0 & \sum_p \mathbb{C}^p_{3j3l}\, h \end{array} \right]. \tag{39}$$

The use of an analytical tangent enables a faster computation as for a numerical tangent. However, a numerical homogenisation remains a computationally expensive technique, which is one of its major drawbacks. It is to mention that this drawback can be minimised by parallelisation of the local solutions.

4 Results

In order to evaluate the proposed multi-scale scheme, a tension, shear, and bending test of a single layer plate, as well of a sandwich plate are proposed. The sandwich plate is composed of three elastic layers, the bottom and top layers are supposed to be stiff; whereas the core material is softer. The restriction to elastic material behaviour is due to simplicity. Non-linear behaviour can be easily included by choice of another UMAT interface.

4.1 Tension Test

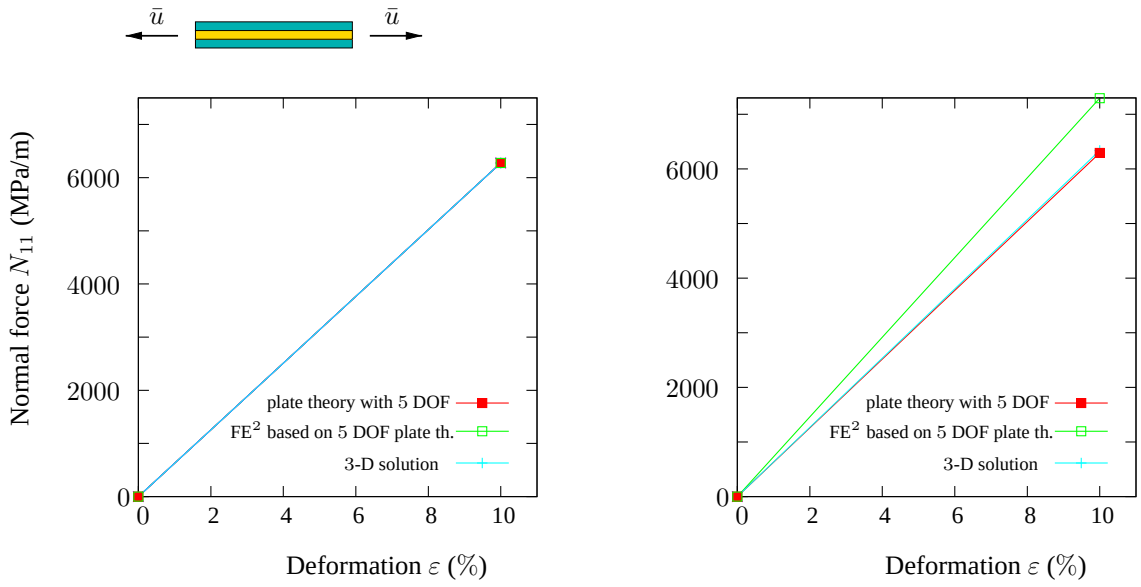

Figure 3: Tension test for a 3 layers material with a zero Poisson's ratio on the left and a non-zero Poisson's ratio on the right

In order to validate our model, a sandwich plate made of 3 elastic layers is computed for a tension test. The FE^2

approach is compared to a fully resolved 3-dimensional FE computation and to the solution of a fully macroscopic solution. In the scope of this academic example, the Poisson's ratio will vary between 0 and 0.4, in order to test the proposed model. As observed in figure 3, if the Poisson's ratios are set to zero for both materials, the results of the reference (here the plate theory or the 3-dimensional problem) and the proposed FE^2 are similar. However, a discrepancy of 15% occurs if the Poisson's ratio of the core material is set to 0.4 and the one of the panels is set to 0.3. The reason for this are the different assumptions done in the multi-scale modelling: on the macroscale, we consider a plate following Mindlin concept, i. e., a plate without thickness change based on a 2-dimensional constitutive law, whereas the mesoscale is a 3-dimensional problem, with a thickness change and with a 3-dimensional constitutive law. It follows an obvious contradiction between the assumptions on the macroscale and on the mesoscale. As a consequence, a plate theory with thickness change would avoid this contradiction and could bring better results. For these reasons, for a non-zero Poisson's ratio, the results can not be the same for a tension test. In the next part, a shear test and later a bending test will be computed and the results compared with the plate theory.

4.2 Shear Test

A simple shear test is computed, as shown in Figure 4, where the results for the proposed multi-scale model, for a plate theory and for a 3-dimensional computation are the same, for the single material, as well as for the sandwich structure. It makes sense, because no transverse deformation occurs for this kind of test.

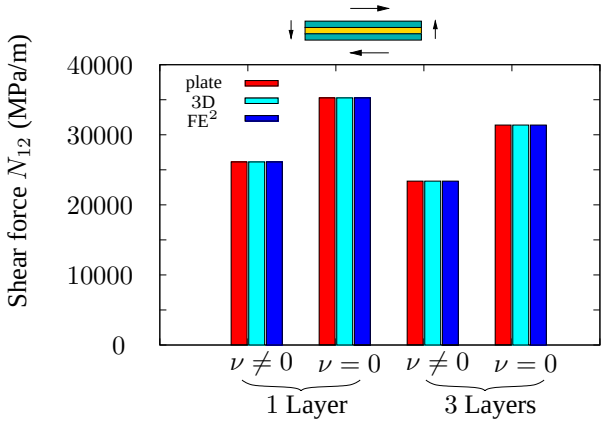

Figure 4: Shear force for a shear test for different cases

4.3 Bending Test

Lastly, a bending test of a single material as well as of a sandwich structure is computed, as represented in Figure 5 for the composite. The distribution of the bending moment is shown in figure 6 for a single layer. The classical

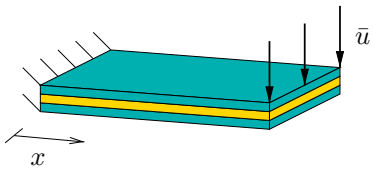

Figure 5: Schematic representation of the computed bending test

plate theory following Mindlin concept with five degrees of freedom is represented in red, whereas the three other curves give the results for the numerical homogenisation, for a mesoscale mesh of 2^3, 3^3, 4^3 and 10^3 elements respectively. For a material with a Poisson's ratio of 0, the convergence is very good; however, for a Poisson's ratio different of 0, the values are converging, but to another value. In the stage of this work, the numerical homogenisation is based on a plate theory which does not take into account any thickness change. For these reasons, we assume that the presented multi-scale model is partly taking the transverse deformations into account (not from the macroscale but from the 3-dimensional problem of the mesoscale), and that this element could explain the

observed discrepancy.

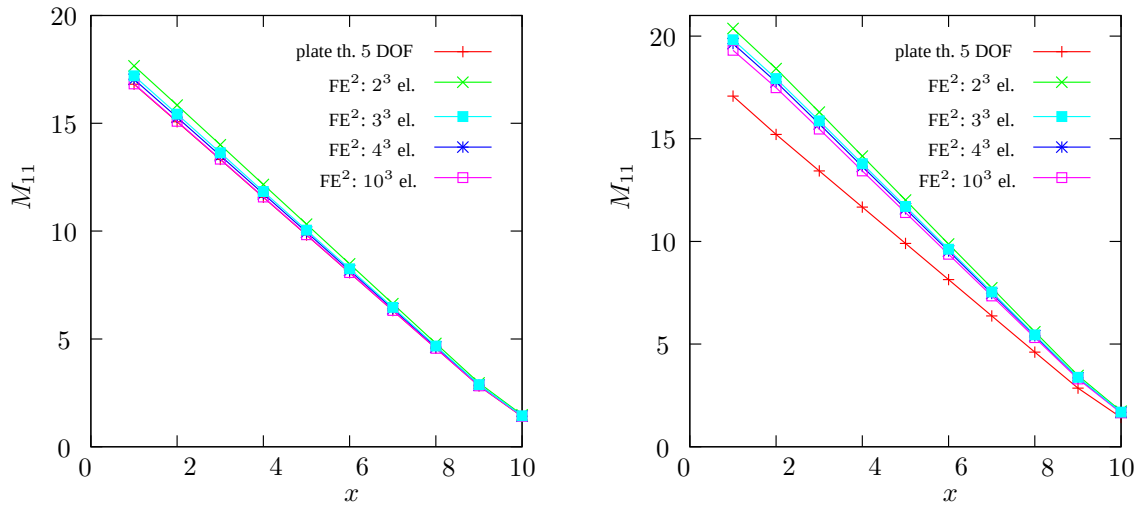

Figure 6: Moment for a single layer, with a Poisson's ratio of 0 (left) and for a Poisson's ratio of 0.35 (right)

A similar bending test is applied for a sandwich structure composed of three layers, as represented in Figure 5; the moment distribution is given in Figure 7. For a Poisson's ratio equal to 0 for both materials, we observe that the error is not to large (between 3% and 8%), but the results are not converging to the results given by the plate theory. The same effect can be observed when the Poisson's ratio is not set to 0, however the errors are larger (from 6% to 11%). At this stage, we formulate the assumption that the considered plate theory on the macroscale is not taking into account any thickness change, and that a plate theory with thickness change could give an accurate result.

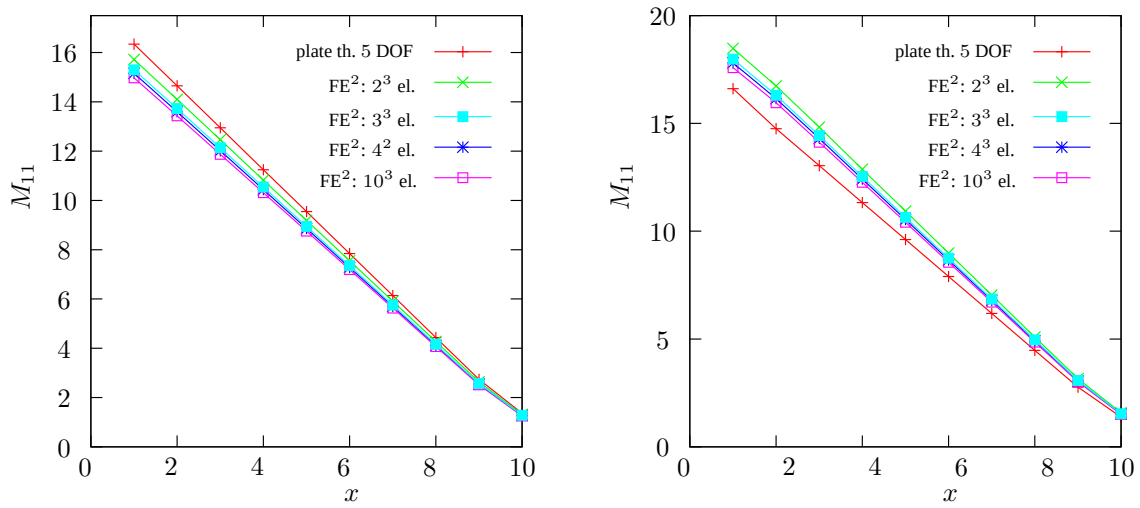

Figure 7: Moment for a sandwich structure, with a Poisson's ratio of 0 for both materials (left) and for a Poisson's ratio average of 0.35 (right)

In Figure 8, the shear stress in the middle of the plate for the single layer, as well as for the considered composite, is represented. For the single material, as well as for the sandwich structure, the difference between the plate theory and the presented model are larger for non-zero Poisson's ratio materials. For a single layer with a zero Poisson's ratio, the error is about 3%. On the contrary, it reaches 20% for a single layer with a Poisson's ratio of 0.35. For the sandwich structure, the error lies between 11% and 15%. Furthermore, we see clearly that the results of the FE^2 model are not converging to the results of the plate theory. For the plate theory of the reference as well as for the plate theory of the macroscale, a shear correction coefficient of $5/6$ (Reissner) is applied; however, we are not awaiting a better result if this factor is changed. At the stage of this work, we give the assumption that

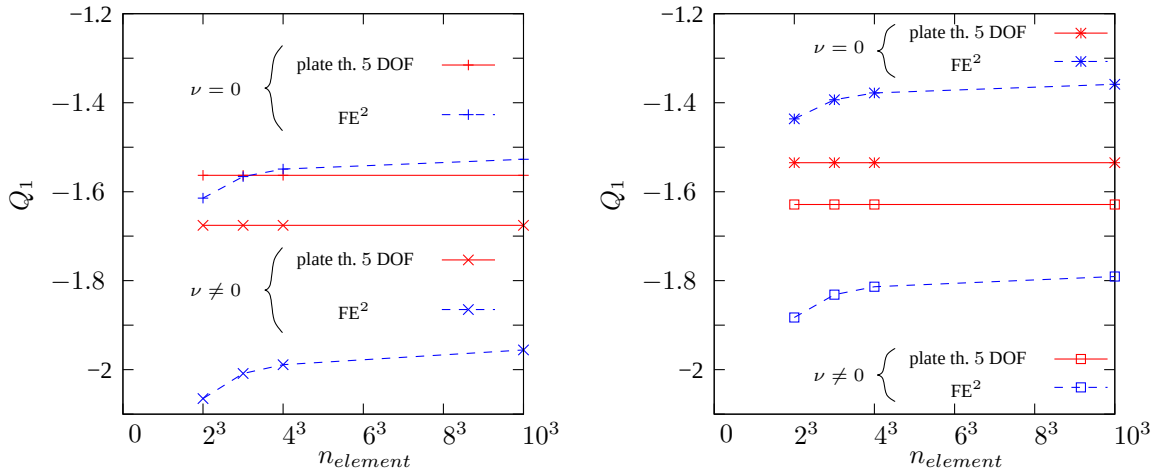

Figure 8: Shear stress for a bending test for a single material (left) and for a sandwich structure (right)

the observed discrepancies derive from the considered plate theory without thickness change. For these reasons, further comparison with classical examples, like for instance the Pagano solution, cf. Pagano (1969) and later developped by Meenen and Altenbach (1998) about the boundary conditions, computed for an anisotropic elastic material behavior, will be developped in a further work dealing with anisotropic plates.

5 Conclusions and Outlook

This paper has proposed a numerical homogenisation method, so-called FE^2, of composites plates. The macroscale is defined as a Finite Element computation of a plate which contains five degrees of freedom. From each Gauss point, the deformations are projected on a 3-dimensional RVE on the mesoscale, where another Finite Element computation is done. The RVE takes the whole thickness of the plate into account and therefore the numerical homogenisation is only made in the two directions parallel to the mid plane, but not in the thickness direction. In the scope of this work, periodic boundary conditions are chosen and a boundary value problem is computed on the mesoscale. In order to identify an analytical tangent, a Multi-Level Newton Algorithm is used and applied to the proposed FE^2 model: the global level consists of the equilibrium equations, whereas the local level deals with the mesoscale. The plate kinematics are used to project the macroscopic deformation to the mesoscale.

The proposed model in computed within tension, shear and bending tests of a single material and of a sandwich structure. For simplicity, the considered materials are elastic, in order to enable a better verification of the model. In a future work, elasto-plastic material behaviour as well as anisotropy will be taken into account.

For the tension test and for the bending test, a discrepancy between the classical plate theory and the proposed multi-scale model occurs for materials with a non-zero Poisson's ratio. We give the assumption that it is caused by the fact that the considered plate theory, for the reference calculations as well as for the numerical homogenisation, does not allow for any thickness change and therefore is unable to consider this kind of effects. As a solution, we have proposed to use a plate theory with thickness change, for instance a plate theory with 7 degrees of freedom; this aspect will be developed in a forthcoming work.

Acknowledgment

The authors thank the German Science Foundation DFG for their financial support under the grant Di 430/11-1.

References

Altenbach, H.: Eine direkt formulierte lineare Theorie für viskoelastische Platten und Schalen. *Ingenieur-Archiv*, 58, (1988), 215–228.

Altenbach, H.; Altenbach, J.; Rikards, R.: *Einführung in die Mechanik der Laminat- und Sandwichtragwerke: Modellierung und Berechnung von Balken und Platten aus Verbundwerkstoffen*. Deutscher Verlag für Grundstoffindustrie, Stuttgart (1996).

Altenbach, J.; Altenbach, H.; Eremeyev, V. A.: On generalized Cosserat-type theories of plates and shells: a short review and bibliography. *Arch. Appl. Mech.*, 80, (2010), 73–92.

Castaneda, P. P.: Second-order homogenization estimates for nonlinear composites incorporating field fluctuations: I–theory. *J. Mech. Phys. Solids*, 50, (2002a), 737–757.

Castaneda, P. P.: Second-order homogenization estimates for nonlinear composites incorporating field fluctuations: Ii–applications. *J. Mech. Phys. Solids*, 50, (2002b), 759–782.

Coenen, E. W. C.; Kouznetsova, V. G.; Geers, M. G. D.: Computational homogenization for heterogeneous thin sheets. *Int. J. Numer. Meth. Eng.*, 83(8-9), (2010), 1180–1205.

Ellsiepen, P.; Diebels, S.: Error-controlled Runge-Kutta time integration in elastoplasticity and viscoplasticity. In: S. Diebels, ed., *Zur Beschreibung komplexen Materialverhaltens: Beiträge anläßlich des 50. Geburtstags von Herrn Prof. Dr.-Ing. Wolfgang Ehlers*, pages 189–206, Institut für Mechanik (Bauwesen) Nr. 01-II-7, Universität Stuttgart (2001).

Ellsiepen, P.; Hartmann, S.: Remarks on the interpretation of current non-linear finite element analysis as differential-algebraic equations. *Int. J. Numer. Meth. Eng.*, 51, (2001), 679–707.

Feyel, F.: Multiscale non linear FE^2 analysis of composite structures: Fiber size effects. *Int. J. Plast.*, 11, (2001), 195–202.

Feyel, F.: A multilevel finite element method (FE^2) to describe the response of highly non-linear structures using generalized continua. *Comp. Meth. Appl. Mech. Eng.*, 192, (2003), 3233–3244.

Feyel, F.; Chaboche, J. L.: FE^2 multiscale approach for modelling the elastoviscoplastic behaviour of long fiber SiC/Ti composite materials. *Comp. Meth. Appl. Mech. Eng.*, 183, (2000), 309–330.

Forest, S.: Mechanics of generalized continua: construction by homogenization. *Int. J. Plast.*, 8, (1998), 39–48.

Forest, S.: Homogenization methods and the mechanics of generalized continua - Part 2. *Theoretical and Applied Mechanics*, 28–29, (2002), 113–143.

Forest, S.; Trinh, D.: Generalised continua and non-homogeneous boundary conditions in homogenisation methods. *Z. Angew. Math. Mech.*, 91, (2011), 90–109.

Geers, M. G. D.; Coenen, E. W. C.; Kouznetsova, V. G.: Multi-scale computational homogenization of structured thin sheets. *Modelling Simul. Mater. Sci. Eng.*, 15, (2007), S393–S404.

Hartmann, S.: A remark on the application of the Newton-Raphson method in non-linear finite element analysis. *Comp. Mech.*, 36, (2005), 100–116.

Hartmann, S.; Quint, K. J.; Hamkar, A. W.: Displacement control in time-adaptive non-linear finite-element analysis. *Z. Angew. Math. Mech.*, 88(5), (2008), 342–364.

Hohe, J.: A direct homogeneisation approach for determination of the stiffness matrix for microheterogeneous plates with application to sandwich panels. *Composites: Part B*, 34, (2003), 615–626.

Jänicke, R.; Diebels, S.: Numerical homogenisation of micromorphic media. *Technische Mechanik*, 30(4), (2010a), 364–373.

Jänicke, R.; Diebels, S.: Requirements on periodic micromorphic media. In: G. A. Maugin; A. Metrikine, eds., *Mechanics of Generalized Continua*, pages 99–108, Springer-Verlag (2010b).

Jänicke, R.; Diebels, S.; GSehlhorst, H.; Düster, A.: Two-scale modelling of micromorphic continua. *Continuum Mech. Therm.*, 21 (4), (2009), 297–315.

Kouznetsova, V. G.: *Computational homogenization for the multi-scale analysis of multi-phase m aterial*. Ph.D. thesis, Technische Universiteit Eindhoven, Eindhoven (2002).

Kouznetsova, V. G.; Brekelmans, W. A. M.; Baaijens, F. P. T.: An approach to micro-macro modeling of heterogeneous materials. *Comp. Mech.*, 27, (2001), 37–48.

Kouznetsova, V. G.; Geers, M. G. D.; Brekelmans, W. A. M.: Multi-scale second-order computational homogenization of multi-phase materials: a nested finite element solution strategy. *Comp. Meth. Appl. Mech. Eng.*, 193, (2004), 5525–5550.

Landervik, M.; Larsson, R.: *Modeling of foams for impact simulation: A higher-order stress-resultant shell formulation based on multiscale homogenization*. Ph.D. thesis, Chalmers University of Technology, Gothenburg (2008).

Larsson, R.; Diebels, S.: A second-order homogenization procedure for multi-scale analysis based on micropolar kinematics. *Int. J. Numer. Meth. Eng.*, 69, (2007), 2485–2512.

Laschet, G.; Jeusette, J. P.; Beckers, P.: Homogenization and pre-integration techniques for multilayer composite and sandwich finite element models. *Int. J. Numer. Meth. Eng.*, 27, (1989), 257–269.

Meenen, J.; Altenbach, H.: Statically equivalent solutions for assessment of refined plate theories. *Mechanics of Composite Materials*, 34 (4), (1998), 331–342.

Pagano, N. J.: Exact solutions for composite laminates in cylindrical bending. *J. Composite Materials.*.

Rabbat, N. B. G.; Sangiovanni-Vincentelli, A. L.; Hsieh, H. Y.: A multilevel newton algorithm with macromodeling and latency for the analysis of large-scale nonlinear circuits in the time domain. *IEES Trans Circuits Sys*, 26 (9), (1979), 733–741.

Reddy, J. N.: On refined theories of composite laminates. *Meccanica*, 25, (1990), 230–238.

Reddy, J. N.: *Mechanics of Laminated Composite Plates, Theory and Analysis*. Department of Mechanical Engineering Texas A&M University College Station, Texas (1997).

Schröder, J.; Miehe, C.; Schotte, J.: Computational homogenization analysis in finite plasticity-simulation of texture development in polycrystalline materials. *Comp. Meth. Appl. Mech. Eng.*.

Suquet, P.: Local and global aspects in the mathematical theory of plasticity. In: *Plasticity Today: Modelling, Methods and Applications*, pages 279–310, Elsevier, London (1985).

Address: Dipl.-Ing. Cécile Helfen and Prof. Dr.-Ing. Stefan Diebels, Chair of Applied Mechanics, Saarland University, Campus A 4.2, Zi. 1.08, D-66123, Saarbrücken, Germany.
email: c.helfen@mx.uni-saarland.de;s.diebels@mx.uni-saarland.de